

Multicomponent radiatively driven stellar winds

III. Radiative-acoustic waves in a two-component wind

J. Krtička^{1,2} and J. Kubát²

¹ Ústav teoretické fyziky a astrofyziky PřF MU, Kotlářská 2, 611 37 Brno, Czech Republic

² Astronomický ústav, Akademie věd České republiky, 251 65 Ondřejov, Czech Republic

Received 5 December 2001 / Accepted 8 March 2002

Abstract. We study the stability of isothermal two-component radiatively driven stellar winds to one-dimensional perturbations larger than the Sobolev length, and radiative-acoustic waves in such stellar winds. We perform linear perturbation analysis in comoving fluid-frames of individual components and obtain the dispersion relation in the common fluid frame. For high density winds the difference between velocities of both components is relatively small and the wind is stable for radiative-acoustic waves discovered originally by Abbott, in accordance with the previous studies of the one-component wind. However, for such high density winds we found new types of waves, including a special case of “frozen-in” wavy patterns. On the other hand, if the velocity difference between wind components is sufficiently large (for low density winds) then the multicomponent stellar wind is unstable even for large-scale perturbations and ion runaway occurs. Thus, isothermal two-component stationary solutions of the radiatively line-driven stellar wind with an abrupt lowering of the velocity gradient are unstable.

Key words. stars: mass-loss – stars: early-type – hydrodynamics – instabilities – waves

1. Introduction

Since the determination of the basic theory of the radiatively driven stellar wind its stability was one of the most fundamental issues to be solved. At the very beginning Lucy & Solomon (1970) concluded that radiatively driven stellar winds are essentially unstable. Contrary to this assertion, Castor et al. (1975) described radiatively driven stellar wind as a smooth and stable steady-state outflow. This contradiction survived when Abbott (1980) showed that the stellar wind described by CAK is stable. On the other hand, MacGregor et al. (1979) and Carlberg (1980) concluded that radiatively driven stellar winds are unstable. This paradox was solved by Owocki & Rybicki (1984). These authors found a general relation which is valid for perturbations both smaller and larger than the Sobolev length, the so called “bridging relation”. The main result of the last paper is that the flow of the line-driven wind is stable for perturbations larger than the Sobolev length (the so-called large-scale perturbations), yielding stable radiative-acoustic waves, which were found by Abbott (1980) and are unstable for perturbations smaller than the Sobolev length, as found by MacGregor et al. (1979) and

Carlberg (1980). The theory of instabilities of radiatively driven stellar wind was further developed by Lucy (1984), Owocki & Rybicki (1985, 1986, 1991), and extended to three-dimensional perturbations by Rybicki et al. (1990). For an introduction to the problem of the stability of a line-driven wind see Rybicki (1987) and Owocki (1992). The existence of instabilities in the wind is important for an X-ray phenomenon because it is usually assumed that X-rays are generated by wind clumping or shocks (e.g. Lucy & White 1980; Lucy 1982; Owocki & Cohen 1999).

On the other hand, it is known that radiatively driven stellar winds have a multicomponent nature (e.g., Springmann & Pauldrach 1992; Babel 1995; Porter & Drew 1995). The stellar radiation is predominantly absorbed by species (typically C, N, O, Fe, etc.) that have much lower density than the rest of the stellar wind, which is composed mainly of hydrogen and helium. However, multicomponent effects are important only for low-density stellar winds. Recently, Krtička & Kubát (2000, 2001a, 2001b, hereafter KK0, KKI, KKII, respectively) computed models of isothermal two-component and non-isothermal three-component radiatively driven stellar winds.

Springmann & Pauldrach (1992) proposed that for low density stellar winds the absorbing component is not able to accelerate the non-absorbing component and that both

Send offprint requests to: J. Krtička,
e-mail: krticka@physics.muni.cz

components decouple. On the other hand, using a model of an isothermal two-component stellar wind, KK0 obtained the surprising result that the components do not decouple and an unexpected decrease in the velocity gradient was found. This effect can be explained by the dependence of the radiative force on the velocity gradient. A question which naturally arises is the stability of such a multicomponent flow.

It is natural to expect that the conclusions about the stability of the one-component wind will be in principal also valid for the two-component flows. Recently, Owocki & Puls (2002, hereafter OP) extended the general one-component stability analysis of Owocki & Rybicki (1984) for the case of a two-component isothermal wind and found that the two-component solution is unstable when the flow is not well coupled. Here we extend Abbott's (1980) calculations to the case of multicomponent flow and study how the overall picture of stable Abbott waves changes in the two-component isothermal stellar wind. The analysis presented in this paper is based on a part of the thesis of Krtićka (2001).

2. Time-dependent hydrodynamic equations for isothermal wind

We assume an isothermal spherically symmetric wind consisting of two components, namely of passive (non-absorbing) hydrogen ions with a mass equal to the proton mass m_p and charge equal to the proton charge q_p and of absorbing ions with mass $A_i m_p$ and charge q_i . Time-dependent radiatively driven stellar wind is then described by the set of hydrodynamic equations, namely with the continuity equations

$$\frac{\partial \rho_p}{\partial t} + \frac{1}{r^2} \frac{\partial}{\partial r} (r^2 \rho_p v_{rp}) = 0, \quad (1a)$$

$$\frac{\partial \rho_i}{\partial t} + \frac{1}{r^2} \frac{\partial}{\partial r} (r^2 \rho_i v_{ri}) = 0, \quad (1b)$$

and with the equations of motion

$$\frac{\partial v_{rp}}{\partial t} + v_{rp} \frac{\partial v_{rp}}{\partial r} = -g + \frac{1}{\rho_p} R_{pi} - \frac{1}{\rho_p} \frac{\partial p_p}{\partial r}, \quad (2a)$$

$$\frac{\partial v_{ri}}{\partial t} + v_{ri} \frac{\partial v_{ri}}{\partial r} = g_i^{\text{rad}} - g - \frac{1}{\rho_i} R_{pi} - \frac{1}{\rho_i} \frac{\partial p_i}{\partial r}. \quad (2b)$$

In these equations v_{rp} , ρ_p , v_{ri} , ρ_i are velocities and densities of passive plasma and accelerated ions, respectively, p_p , p_i are partial gas pressures of each component ($p_p = a_p^2 \rho_p$, $p_i = a_i^2 \rho_i$), isothermal sound velocities are $a_p^2 = kT/m_p$ and $a_i^2 = kT/m_i$, $g = G\mathfrak{M}(1 - \Gamma)/r^2$ is the gravitational acceleration (corrected for absorption by free electrons) acting on each component (G and \mathfrak{M} are the gravitational constant and stellar mass, respectively, Γ is the Eddington factor accounting for the absorption on free electrons) and g_i^{rad} is the radiative acceleration acting on absorbing ions. We take the radiative acceleration in the form

$$g_i^{\text{rad}} = \frac{1}{\mathfrak{M}_i} \frac{\sigma_e L}{4\pi r^2 c} f \left(\frac{n_e/W}{10^{11} \text{cm}^{-3}} \right)^\delta k \left(\frac{\mathfrak{M}_i}{\sigma_e v_{th} \rho_i} \frac{dv_{ri}}{dr} \right)^\alpha, \quad (3)$$

with force multipliers k , α , δ after Abbott (1982). Here f is the finite disk correction factor (Pauldrach et al. 1986; Friend & Abbott 1986), n_e is the electron density (we set $n_e = n_p$), and W is stellar dilution factor. Here we have introduced the factor \mathfrak{M}_i (which is the ratio of the absorbing ion density to the passive plasma density in a stellar atmosphere) to account for radiative acceleration acting directly on ions (see KK0).

Frictional force (per unit volume) R_{pi} acting between both components has following form (Springmann & Pauldrach 1992):

$$R_{pi} = -n_p n_i k_{pi} G(x_{pi}), \quad (4)$$

where n_p and n_i are number densities of passive plasma and absorbing ions. The friction coefficient k_{pi} is given by

$$k_{pi} = \frac{4\pi \ln \Lambda q_p^2 q_i^2}{kT} \frac{v_{rp} - v_{ri}}{|v_{rp} - v_{ri}|}, \quad (5)$$

where $\ln \Lambda$ is the Coulomb logarithm, $G(x)$ is the so-called Chandrasekhar function (see Springmann & Pauldrach 1992, KK0 and Fig. 1 for the shape of this function). The argument x_{pi} of the Chandrasekhar function in Eq. (4) is proportional to the ratio of the drift velocity $|v_{rp} - v_{ri}|$ to the thermal velocity v_{th} , namely

$$x_{pi} = \sqrt{A_{pi}} \frac{|v_{rp} - v_{ri}|}{v_{th}}, \quad (6)$$

where $A_{pi} = A_p A_i / (A_p + A_i)$ is a reduced atomic mass.

3. Radiative-acoustic waves

Similarly to Abbott (1980), we keep the equations locally linear and we study waves in comoving fluid frames of individual components. Since the velocities of the components are different, we start by using two different fluid frames (one for each component). Thus, we use comoving fluid frames of non-absorbing and absorbing components

$$r_p = r' - v_p(r')t, \quad (7a)$$

$$r_i = r' - v_i(r')t, \quad (7b)$$

instead of the frame of the static observer r' (note that both comoving fluid-frames are chosen to be local inertial fluid frames). Here both r_p and r_i are radial coordinates. We assume that the wind is perturbed from its original steady-state and that the perturbed quantities do not change the density scale height. The perturbed quantities are denoted by $\delta \rho_p$, δv_p , $\delta \rho_i$, and δv_i .

The time-dependent continuity equations to the first order are

$$\frac{\partial \delta \rho_p}{\partial t_p} + \rho_{0,p} \frac{\partial \delta v_p}{\partial r_p} = 0, \quad (8a)$$

$$\frac{\partial \delta \rho_i}{\partial t_i} + \rho_{0,i} \frac{\partial \delta v_i}{\partial r_i} = 0, \quad (8b)$$

and two-component time-dependent linearized momentum equations are

$$\frac{\partial \delta v_p}{\partial t_p} = -\frac{a_p^2}{\rho_{0,p}} \frac{\partial \delta \rho_p}{\partial r_p} + \frac{R_{pi}}{\rho_{0,p}} \frac{G'(\Delta v_0)}{G(\Delta v_0)} (\delta v_i - \delta v_p), \quad (9a)$$

$$\begin{aligned} \frac{\partial \delta v_i}{\partial t_i} &= -\frac{a_i^2}{\rho_{0,i}} \frac{\partial \delta \rho_i}{\partial r_i} + \partial_{v'} g^{\text{rad}} \frac{\partial \delta v_i}{\partial r_i} \\ &\quad - \frac{R_{pi}}{\rho_{0,i}} \frac{G'(\Delta v_0)}{G(\Delta v_0)} (\delta v_i - \delta v_p), \end{aligned} \quad (9b)$$

where the subscript 0 denotes unperturbed quantity in the observer's frame, the velocity difference is $\Delta v_0 = v_{0,i} - v_{0,p}$, $G(\Delta v_0) = G(x_{ip})$, $G'(\Delta v_0) = \partial G(\Delta v_0) / \partial \Delta v_0$ and $\partial_{v'} g^{\text{rad}} = \partial g_i^{\text{rad}} / \partial (\partial v_{0,i} / \partial r_i)$. We neglected gravity and density stratification in the momentum equation and assumed that the radiative force depends only on the velocity gradient. In these equations we simply suppose a Galilean transformation of coordinates for which $t_p = t_i = t$. We distinguish between t_p and t_i to emphasize the difference in partial derivatives with respect to time. During calculation of $\partial / \partial t_p$ one should keep r_p constant and, similarly, for $\partial / \partial t_i$ one should keep r_i constant. The Galilean transformation also implies that the velocity difference Δv_0 and perturbations of velocities and densities $\delta \rho_p$, $\delta \rho_i$, δv_p and δv_i are the same in both inertial frames. We neglected density perturbations of the radiative and frictional forces. This is consistent with the calculations of Abbott (1980) where density perturbations of the radiative force have been also neglected. Justification of this neglect can be found, e.g., in the Appendix of OP.

Taking a partial derivative of the Eq. (8b) with respect to r_p and substituting it for the partial derivative of the Eq. (9a) with respect to t_p gives

$$\frac{\partial^2 \delta v_p}{\partial t_p^2} = a_p^2 \frac{\partial^2 \delta v_p}{\partial r_p^2} + \frac{R_{pi}}{\rho_{0,p}} \frac{G'(\Delta v_0)}{G(\Delta v_0)} \left[\frac{\partial \delta v_i}{\partial t_p} - \frac{\partial \delta v_p}{\partial t_p} \right]. \quad (10a)$$

Similarly, the partial derivative of the Eq. (8a) with respect to r_i and subsequent substitution to the derived Eq. (9b) with respect to t_i gives

$$\begin{aligned} \frac{\partial^2 \delta v_i}{\partial t_i^2} &= a_i^2 \frac{\partial^2 \delta v_i}{\partial r_i^2} + \partial_{v'} g^{\text{rad}} \frac{\partial^2 \delta v_i}{\partial r_i \partial t_i} \\ &\quad - \frac{R_{pi}}{\rho_{0,i}} \frac{G'(\Delta v_0)}{G(\Delta v_0)} \left[\frac{\partial \delta v_i}{\partial t_i} - \frac{\partial \delta v_p}{\partial t_i} \right]. \end{aligned} \quad (10b)$$

We obtained two differential equations for velocity perturbations of both components. Unfortunately, these equations are written in *different* fluid frames. To proceed further, we have to rewrite these equations in one common frame. We selected the fluid frame of accelerated ions. From the relations

$$r_i = r_p - \Delta v_0 t_p, \quad (11a)$$

$$t_i = t_p, \quad (11b)$$

it follows that

$$\frac{\partial}{\partial r_p} = \frac{\partial}{\partial r_i}, \quad (12a)$$

$$\frac{\partial}{\partial t_p} = \frac{\partial}{\partial t_i} - \Delta v_0 \frac{\partial}{\partial r_i}, \quad (12b)$$

$$\frac{\partial^2}{\partial r_p^2} = \frac{\partial^2}{\partial r_i^2}, \quad (12c)$$

$$\frac{\partial^2}{\partial t_p^2} = \frac{\partial^2}{\partial t_i^2} - 2\Delta v_0 \frac{\partial^2}{\partial t_i \partial r_i} + \Delta v_0^2 \frac{\partial^2}{\partial r_i^2}. \quad (12d)$$

Thus, we rewrite Eq. (10a) as

$$\begin{aligned} \frac{\partial^2 \delta v_p}{\partial t_i^2} - 2\Delta v_0 \frac{\partial^2 \delta v_p}{\partial t_i \partial r_i} + \Delta v_0^2 \frac{\partial^2 \delta v_p}{\partial r_i^2} &= a_p^2 \frac{\partial^2 \delta v_p}{\partial r_i^2} \\ &\quad + \frac{R_{pi}}{\rho_{0,p}} \frac{G'(\Delta v_0)}{G(\Delta v_0)} \left(\frac{\partial}{\partial t_i} - \Delta v_0 \frac{\partial}{\partial r_i} \right) (\delta v_i - \delta v_p). \end{aligned} \quad (13)$$

We assume a solution in the form of propagating waves, which in the reference frame of ions are

$$\delta v_p = V_p \exp [i (\omega_p t_i - \kappa_p r_i)], \quad (14a)$$

$$\delta v_i = V_i \exp [i (\omega_i t_i - \kappa_i r_i)]. \quad (14b)$$

The amplitudes V_p , V_i are generally complex to account for phase shifts, and, since we are doing linear analysis, they depend neither on r_i nor on t_i . Similarly, ω_p , ω_i , κ_p , and κ_i are independent of r_i and t_i . Substituting from (14) into the wave Eqs. (13) and (10b) we obtain a system of equations

$$\begin{aligned} &\left[(\omega_p + \Delta v_0 \kappa_p)^2 V_p - a_p^2 \kappa_p^2 V_p \right. \\ &\quad \left. - i \frac{R_{pi}}{\rho_{0,p}} \frac{G'(\Delta v_0)}{G(\Delta v_0)} (\omega_p + \Delta v_0 \kappa_p) V_p \right] e^{i(\omega_p t - \kappa_p r_i)} \\ &= -i \frac{R_{pi}}{\rho_{0,p}} \frac{G'(\Delta v_0)}{G(\Delta v_0)} (\omega_i + \Delta v_0 \kappa_i) V_i e^{i(\omega_i t - \kappa_i r_i)}, \end{aligned} \quad (15a)$$

$$\begin{aligned} &\left[\omega_i^2 V_i - a_i^2 \kappa_i^2 V_i + \kappa_i \partial_{v'} g^{\text{rad}} \omega_i V_i \right. \\ &\quad \left. - i \frac{R_{pi}}{\rho_{0,i}} \frac{G'(\Delta v_0)}{G(\Delta v_0)} \omega_i V_i \right] e^{i(\omega_i t - \kappa_i r_i)} \\ &= -i \frac{R_{pi}}{\rho_{0,i}} \frac{G'(\Delta v_0)}{G(\Delta v_0)} \omega_p V_p e^{i(\omega_p t - \kappa_p r_i)}. \end{aligned} \quad (15b)$$

We are looking for a non-trivial solution of Eqs. (15), i.e. a solution with $V_i \neq 0$, $V_p \neq 0$ for arbitrary t , r_i . Equation (15a) can be rewritten as

$$\tilde{A}_{pp} V_p e^{i(\omega_p t - \kappa_p r_i)} = \tilde{A}_{pi} V_i e^{i(\omega_i t - \kappa_i r_i)}$$

or

$$V_p = \frac{\tilde{A}_{pi}}{\tilde{A}_{pp}} \exp [i (\omega_i - \omega_p) t - i (\kappa_i - \kappa_p) r_i] V_i.$$

Because V_p , V_i , \tilde{A}_{pp} and \tilde{A}_{pi} do not depend on t and r_i , the last equation can be fulfilled only if

$$\omega_p t - \kappa_p r_i = \omega_i t - \kappa_i r_i \quad (16)$$

holds for any t , r_i (the same conclusion can be obtained from Eq. (15b)). Thus, wavenumbers and frequencies of both components are the same,

$$\kappa_i = \kappa_p, \quad (17a)$$

$$\omega_i = \omega_p. \quad (17b)$$

Dividing Eqs. (15) by the exponential factor and denoting $\kappa \equiv \kappa_p$ and $\omega \equiv \omega_p$ we can rewrite the remaining system of equations as

$$(\omega + \Delta v_0 \kappa)^2 V_p = a_p^2 \kappa^2 V_p - i \frac{R_{pi}}{\rho_{0,p}} \frac{G'(\Delta v_0)}{G(\Delta v_0)} \times (\omega + \Delta v_0 \kappa) (V_i - V_p), \quad (18a)$$

$$\omega^2 V_i = a_i^2 \kappa^2 V_i - \kappa \partial_{v'} g^{\text{rad}} \omega V_i + i \frac{R_{pi}}{\rho_{0,i}} \frac{G'(\Delta v_0)}{G(\Delta v_0)} \omega (V_i - V_p). \quad (18b)$$

This system of equations can be rewritten in the matrix form as

$$\mathbf{A}\mathbf{V} = 0, \quad (19)$$

where the vector $\mathbf{V} = (V_p, V_i)^T$ and individual elements of the matrix \mathbf{A} are

$$A_{pp} = \omega^2 + 2\Delta v_0 \kappa \omega + \Delta v_0^2 \kappa^2 - a_p^2 \kappa^2 - i P_p (\omega + \Delta v_0 \kappa), \quad (20a)$$

$$A_{pi} = i P_p (\omega + \Delta v_0 \kappa), \quad (20b)$$

$$A_{ip} = i P_i \omega, \quad (20c)$$

$$A_{ii} = \omega^2 - a_i^2 \kappa^2 + \kappa \partial_{v'} g^{\text{rad}} \omega - i P_i \omega, \quad (20d)$$

where

$$P_p = \frac{R_{pi}}{\rho_{0,p}} \frac{G'(\Delta v_0)}{G(\Delta v_0)}, \quad (21a)$$

$$P_i = \frac{R_{pi}}{\rho_{0,i}} \frac{G'(\Delta v_0)}{G(\Delta v_0)}. \quad (21b)$$

Equation (19) has a non-zero solution only if

$$|\mathbf{A}| = 0, \quad (22)$$

which is the dispersion relation. Generally, it has a complicated form and we will solve it numerically. However, in order to better understand the general dispersion relation we shall first find an analytical solution for some simpler specific cases.

3.1. Abbott waves

Let us assume that the velocity amplitudes of the components p and i are nearly equal ($V_i \approx V_p$) and that the phase velocity of the wave is much larger than the drift velocity ($\omega/k \gg \Delta v_0$), i.e. the flow is well coupled. Then the terms containing Δv_0 in the Eq. (18a) can be neglected. These conditions mimic the one-component case, for which Abbott (1980) obtained stable radiative-acoustic waves, the so-called Abbott waves. We may expect that for

well coupled high density winds the two-component waves are similar to the Abbott waves. Indeed, summing dispersion relations (18) the imaginary frictional term vanishes, and we obtain the dispersion equation in the form of two-component Abbott waves

$$(\omega^2 - a_p^2 \kappa^2) \rho_{0,p} + (\omega^2 + \omega \kappa \partial_{v'} g^{\text{rad}} - a_i^2 \kappa^2) \rho_{0,i} = 0. \quad (23)$$

This equation corresponds to the one-component dispersion relation and thus justifies the condition used by KK0 to fix the mass-loss rate. Then solving the Eq. (23) for ω , the dispersion relation takes the form of

$$\omega = \kappa \left[-\frac{1}{2} \frac{\rho_{0,i}}{\rho_{0,p}} \partial_{v'} g^{\text{rad}} \pm \sqrt{\left(\frac{1}{2} \frac{\rho_{0,i}}{\rho_{0,p}} \partial_{v'} g^{\text{rad}} \right)^2 + a_p^2} \right], \quad (24)$$

where we neglected the density of absorbing ions compared to the passive plasma density. Note that Eq. (24) is the same as Eq. (47) of Abbott (1980), since we used a modified definition of the driving force Eq. (3) to account for the fact that only the ionic gas is line-driven. Apparently, ω is real and thus this mode is neither unstable nor damped. There are two branches of ω corresponding to forward and backward waves, both depending linearly on wavenumber. Note, however, that the general dispersion relation derived by Owocki & Rybicki (1984) for the one-component flow allows for instabilities for short-wavelength perturbations.

The point where the velocity of backward waves is equal to the wind velocity is called the critical point. The flow above the critical point cannot communicate with the wind base. Thus, early-type stars are surrounded by the critical surface, that separates two different domains of the stellar wind. Feldmeier & Shlosman (2000) aptly compare this situation to the cosmic censorship hypothesis. The result that the multicomponent nature of the wind does not alter the Abbott waves is important because these waves determine the mass-loss of the CAK wind (Feldmeier & Shlosman 2001).

Finally, in the case when the gas-pressure term a_p^2 can be neglected, the dispersion relation (24) corresponds to the ω_+ mode of OP, namely

$$\omega_+ \approx -\kappa \frac{\rho_{0,i}}{\rho_{0,p}} \partial_{v'} g^{\text{rad}}. \quad (25)$$

We denoted this mode in accordance with OP as ω_+ although this mode is upstream. Note that Eq. (24) has another solution for $a_p = 0$, namely $\omega = 0$.

3.2. Purely ionic Abbott waves

In the case when $|V_i| \gg |V_p|$ we can obtain from the Eq. (18b) the dispersion relation in the form of Abbott waves in absorbing ions

$$\omega^2 = a_i^2 \kappa^2 - \omega \kappa \partial_{v'} g^{\text{rad}} + i \frac{R_{pi}}{\rho_{0,i}} \frac{G'(\Delta v_0)}{G(\Delta v_0)}. \quad (26)$$

We will study such waves in the case when the pressure term $a_i^2 \kappa^2$ in the dispersion Eq. (26) can be neglected.

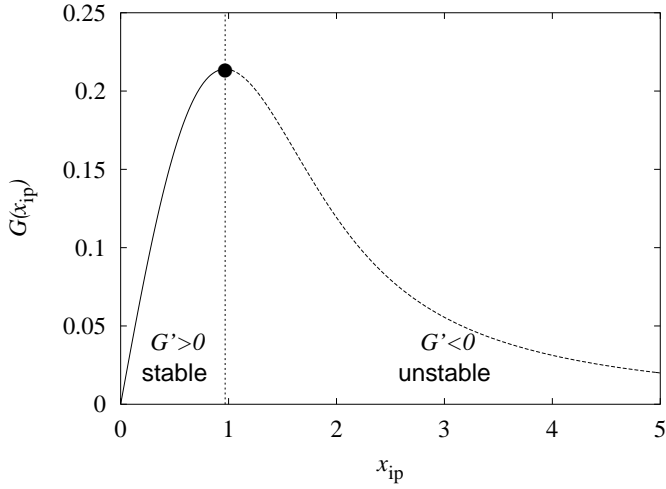


Fig. 1. The run of Chandrasekhar function (note, that Eq. (6) yields $x_{\text{ip}} \sim \Delta v_0$). When the flow is well coupled, $x_{\text{ip}} \lesssim 0.97$, $G'(\Delta v_0) > 0$ and the wind is stable. When the drift velocity is large, $x_{\text{ip}} \gtrsim 0.97$, $G'(\Delta v_0) < 0$ and the wind is unstable. Note that the point $x_{\text{ip}} \approx 0.97$ corresponds to the maximum of G .

In this case, the dispersion relation has a form, which corresponds to the ω_- mode of OP,

$$\omega_- = -\kappa \partial_{v'} g^{\text{rad}} + i \frac{R_{\text{pi}}}{\rho_{0,i}} \frac{G'(\Delta v_0)}{G(\Delta v_0)}. \quad (27)$$

The real part of ω_- depends on κ linearly, whereas the imaginary part does not depend on κ . Due to the presence of the imaginary term in Eq. (27) such waves are damped in the case when $G'(\Delta v_0) > 0$. For clearness we plotted the shape of the Chandrasekhar function in Fig. 1. Thus, if the wind is coupled [when the drift velocity is lower than the thermal velocity or, more precisely, when the Chandrasekhar function is a rising function of Δv_0 ($G'(\Delta v_0) > 0$)], the wind is stable for this type of wave. On the other hand, when the Chandrasekhar function $G(x)$ is decreasing ($G'(\Delta v_0) < 0$), the wind is not stable for the mentioned above perturbations, and this mode leads to ion runaway.

Physical reasons for such an instability are straightforward. If the Chandrasekhar function is before its maximum (as function of Δv_0), then the increase of the velocity difference between velocities of ions and passive plasma enhances the frictional force, which finally tends to lower the velocity difference, yielding a stable flow. In the opposite case (if the velocity difference is larger than that corresponding to the maximum of the Chandrasekhar function) the increase in the velocity difference lowers the frictional force, which allows for additional increase in the velocity difference. Such a two-component flow is clearly unstable. This is the effect of ion runaway (see also Springmann & Pauldrach 1992, OP).

At a first glance there might exist similar acoustic waves in the non-absorbing component. However, this is not the case, because the imaginary term in Eq. (18b) is larger than in Eq. (18a) and thus Eq. (18b) does not

allow $|V_{\text{p}}| \gg |V_{\text{i}}|$. Therefore there are no acoustic counterparts of such waves in a non-absorbing component, i.e. there are no passive plasma waves for which the condition $|V_{\text{p}}| \gg |V_{\text{i}}|$ is valid.

3.3. Zero frictional force

To complete the list of simplified cases, we have also to mention the hypothetical case when interaction between the components vanishes. If both flow components do not influence each other, i.e. if the frictional force is zero, then the system of Eqs. (15) does not implicate that the frequencies and wavenumbers of both components are equal. Instead of the system of dispersion relations (18) we obtain two independent relations for each wind component

$$(\omega_{\text{p}} + \Delta v_0 \kappa_{\text{p}})^2 - a_{\text{p}}^2 \kappa_{\text{p}}^2 = 0, \quad (28a)$$

$$\omega_{\text{i}}^2 - a_{\text{i}}^2 \kappa_{\text{i}}^2 + \kappa_{\text{i}} \partial_{v'} g^{\text{rad}} \omega_{\text{i}} = 0. \quad (28b)$$

The dispersion relation of the nonabsorbing component (28a) describes ordinary isothermal sound waves and the dispersion relation of the ionic component (28b) describes stable Abbott waves of absorbing ions.

Note that a similar result of independent waves can be obtained for the maximum of the Chandrasekhar function, for which $G'(\Delta v_0) = 0$ and the interaction terms in Eqs. (18) vanish as for the case of zero frictional force.

4. Numerical results

The simplified calculations presented in Sects. 3.1 and 3.2 can help us to better understand the behavior of individual branches of the general dispersion relation (22). These calculations have been done numerically. To study the individual branches of the dispersion relation we solved numerically Eq. (22) using the procedure CPOLY of Jenkins & Traub (1970).

Moreover, solving Eqs. (18a) or (18b) for given ω and κ we obtain the relation between wind amplitudes

$$V_{\text{i}} = -\frac{A_{\text{pp}}}{A_{\text{pi}}} V_{\text{p}} \quad (29a)$$

or, equivalently,

$$V_{\text{i}} = -\frac{A_{\text{ip}}}{A_{\text{ii}}} V_{\text{p}}. \quad (29b)$$

4.1. Stable wind for ionic Abbott waves

First, we shall study the case of the star ϵ Ori described in KK0. This star has a relatively dense wind, so the drift velocity between both components is low compared to the thermal speed of hydrogen and thus this wind should be stable for ionic Abbott waves because $G'(\Delta v_0) > 0$ in this case (cf. Sect. 3.2). To be specific, we shall study the dispersion relation in the point where $v_{\text{r}} \approx 0.3 v_{\infty}$. This choice does not influence the overall picture of our results, however.

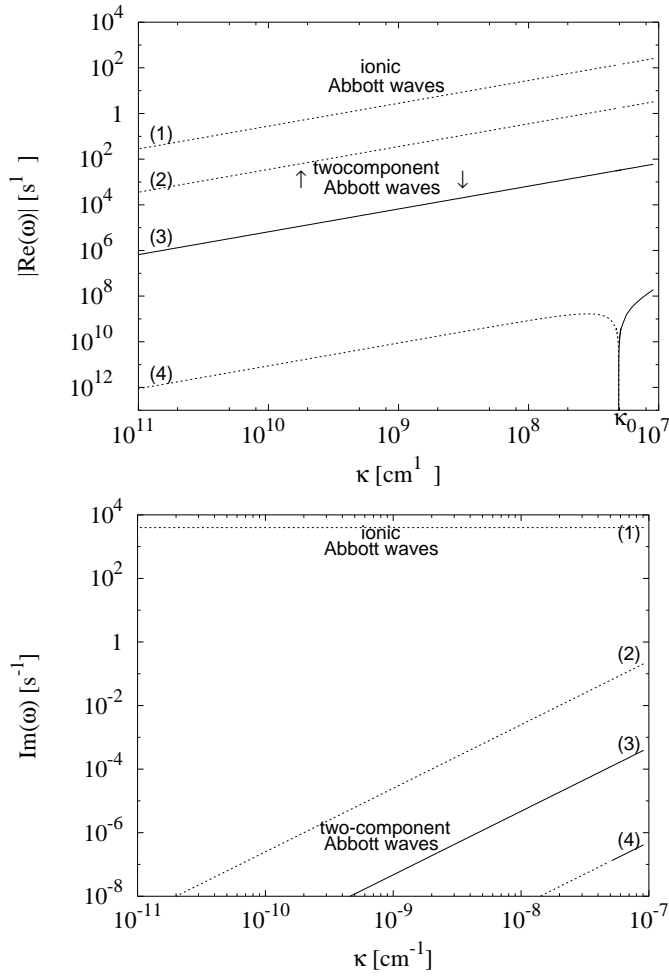


Fig. 2. Individual branches of the dispersion relation for the point where $v_r \approx 0.3 v_\infty$ in the dense wind for a specific case of ϵ Ori. *Upper panel:* real roots of ω . Solid line represents a forward wave, dashed ones backward waves. Note that the real part of branch denoted as (4) changes its sign and for $\kappa = \kappa_0$ is the real part of frequency ω zero. *Lower panel:* imaginary roots of ω , all waves are damped. As in the upper panel, solid and dashed lines denote forward and backward waves, respectively. Real and imaginary parts of individual roots are denoted using the same numbers.

Resulting dispersion relations are displayed in Fig. 2. Real parts of branches show linear dispersion relations, as was predicted in Eqs. (24) and (27). The real branches of Abbott waves (two middle straight lines in both panels of Fig. 2 denoted by (2) and (3)) in the two-component case are essentially the same as in the one-component case (cf. Abbott 1980). From the corresponding imaginary parts of these two-component Abbott waves, it follows that these waves are damped only marginally. If we extend the calculations to $\kappa > 10^{-7} \text{ cm}^{-1}$ we could in principle obtain a larger damping, but these values are beyond the region of validity of the assumption of perturbations larger than the Sobolev length. We also calculated the relation between wave amplitudes V_i and V_p of absorbing and non-absorbing components using Eq. (29a). This calculation confirmed the assumption used in Sect. 3.1 for calculation

of two-component Abbott waves that wave amplitudes for these waves are nearly the same.

The largest imaginary branch corresponding to the ionic Abbott waves (upper straight line in both panels of Fig. 2) does not depend on κ (see Eq. (27)). Clearly, according to previous results, such waves are heavily damped. Moreover, the calculation of the relation between V_i and V_p confirmed that $|V_i| \gg |V_p|$ for these waves (cf. Sect. 3.2).

However, a new type of slow wave appeared. It is described by the lower curves in both panels of Fig. 2 (denoted as (4)). The real parts of the dispersion relations show almost linear dependence with the exception of the region where it passes through the value of $\Re(\omega) = 0$. Consequently, this solution corresponds to both forward and backward waves, which are stable and only marginally damped. The case of $\Re(\omega) = 0$ deserves special attention. It corresponds to a static wavy structure in the comoving frame, so in the observer frame this structure resembles almost stable outflowing “frozen-in” wavy patterns of the characteristic size of $\kappa_0^{-1} \approx 10^7 \text{ cm}$ for this specific case (note that κ_0 is the wavenumber for which $\Re(\omega) = 0$).

In addition, calculations showed that the value of wavenumber κ_0 (for which $\Re(\omega) = 0$) depends on the distance from the star. At the base of the wind, the value of κ_0 is lower, $\kappa_0 \approx 10^{-6} \text{ cm}^{-1}$, implying the possible characteristic pattern size of the order of 10^6 cm whereas in the outer parts of the wind $\kappa_0 \approx 10^{-10} \text{ cm}^{-1}$, yielding the characteristic pattern size of the order of 10^{10} cm .

For this new type of wave we can obtain an approximate analytical dispersion relation. Calculations showed that due to the low value of ω for these waves, all terms in the dispersion relation (22) can be neglected except constant terms and terms linear in ω . Further neglect of all terms that do not significantly influence this type of wave leads to the dispersion relation in the form of

$$\omega (-a_p^2 \partial_{v'} g^{\text{rad}} \kappa + i a_p^2 P_i) + \kappa^2 a_p^2 a_i^2 + i \Delta v_0 P_p a_i^2 \kappa \approx 0. \quad (30)$$

The condition $\Re(\omega) = 0$ can be now written as

$$\kappa^2 a_p^2 \partial_{v'} g^{\text{rad}} - \Delta v_0 P_p P_i \approx 0 \quad (31)$$

from which we can obtain the equation for κ_0 in the form of

$$\kappa_0 \approx \frac{1}{a_p} \sqrt{\frac{\Delta v_0 P_p P_i}{\partial_{v'} g^{\text{rad}}}}. \quad (32)$$

However, we must keep in mind that our analysis was only linear; taking into account the nonlinear effects may change this promising picture, similarly to the case of one-component Abbott waves which become unstable if the second order effects are taken into account (Feldmeier 1998).

4.2. Unstable wind for ionic Abbott waves

Next, we study a model of a B5 star with artificially enhanced effect of friction ($q_i = 4.8 q_p$, see KK0) where the

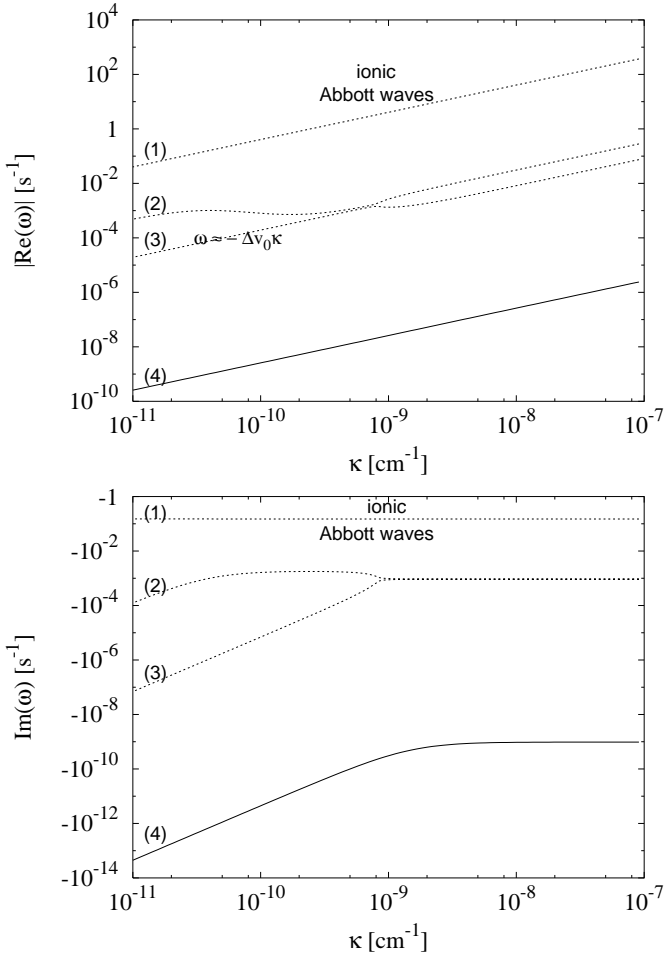


Fig. 3. Dispersion relation for the point $r = 2.4 R_*$ in the wind of a B5 star with $q_i = 4.8q_p$. *Upper panel:* real roots of ω . Solid line represents a forward wave, dashed ones backward waves. The relation approximately corresponding to the dispersion relation $\omega = -\Delta v_0 \kappa$ (see Eq. (33)) is denoted. *Lower panel:* imaginary roots of ω , all waves lead to an instability. As in the upper panel, solid and dashed lines denote forward and backward waves, respectively. Real and imaginary parts of individual roots are denoted using the same numbers.

multicomponent nature of the flow plays an important role and leads to lower outflow velocity than in a one-component case. Here we study the dispersion relation at the point $r = 2.4 R_*$ where the drift velocity between both components exceeds the value corresponding to the maximum of the Chandrasekhar function and, therefore, $G'(\Delta v_0) < 0$ (see Fig. 1).

The dispersion relations displayed in Fig. 3 substantially differ from the previous case. Consistent with the simplified considerations in Sect. 3.2, the imaginary parts of all roots are negative and therefore the flow is unstable. The branch with the largest absolute value of both real and imaginary parts corresponds to the ionic Abbott waves. According to the Eq. (27), the real part of this branch depends on κ linearly whereas the imaginary part does not depend on κ .

A natural question arises: Where have the two-component Abbott waves disappeared to? However, the simplified calculations yielding the two-component Abbott waves (see Sect. 3.1) are not valid in this case, because the velocity difference Δv_0 cannot be simply neglected. On the other hand, the dispersion relation (22) can be approximately fulfilled if the term $\omega + \Delta v_0 \kappa$ vanishes. This conclusion can be simply justified because the dispersion relation (22) can be rewritten as

$$A_{pp}A_{ii} - A_{pi}A_{ip} = 0$$

and when $\omega + \Delta v_0 \kappa = 0$ then the A_{pi} term vanishes identically and A_{pp} vanishes if the pressure term $a_p^2 \kappa^2$ is negligible (see Eqs. (20a) and (20b)). The linear dispersion relation

$$\omega = -\Delta v_0 \kappa \quad (33)$$

is visible in Fig. 3 (note that $\Delta v_0 \approx 10^6 \text{ cm s}^{-1}$).

4.3. On the stability of the B5 star wind model

Nevertheless, the analysis presented in Sect. 4.2 does not mean that the *entire* wind is unstable for the mentioned above two-component instability. Since stability depends on the sign of $G'(\Delta v_0)$ which varies throughout the flow, there are regions where the wind is stable and regions where the wind is unstable. This situation is depicted in Fig. 4.

Near the stellar surface the wind is well coupled ($\omega/k \gg \Delta v_0$), the Chandrasekhar function is below its maximum (as a function of the velocity difference), $G'(\Delta v_0) > 0$ and the wind is stable (see Eq. (27)).

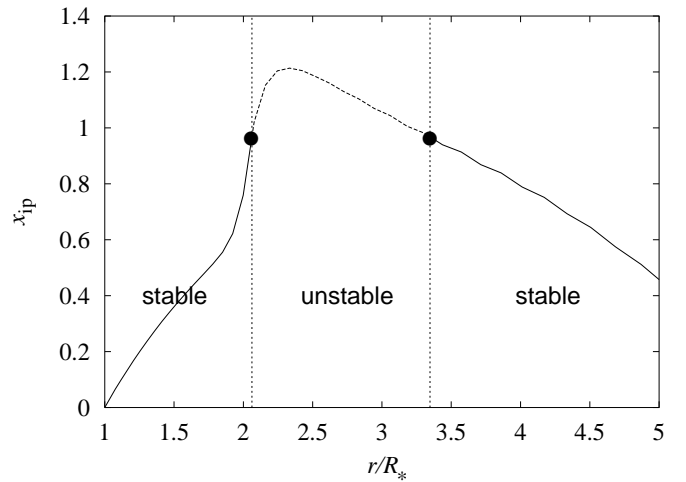


Fig. 4. The stability of the wind of a B5 star with $q_i = 4.8q_p$. At the base of the wind $x_{ip} \lesssim 0.97$ (note that the value $x_{ip} \approx 0.97$ approximately corresponds to the maximum of the Chandrasekhar function, see Fig. 1) and the wind is stable. In the outer parts the density decreases, the Chandrasekhar function reaches its maximum and $x_{ip} \gtrsim 0.97$, the wind is not stable. In the outermost parts of the wind is $x_{ip} \lesssim 0.97$ again and the wind is stable.

This conclusion was justified by numerical calculations at the point where $v_{\text{rp}} \approx 4a_{\text{p}}$ (the dispersion relation obtained resembles that in Fig. 2).

The wind is accelerated downstream, its density decreases and the velocity difference Δv_0 between both components increases. However, such low density wind reaches the point where the maximum of the Chandrasekhar function is reached and the absorbing component is not able to accelerate the passive component sufficiently. Due to the functional dependence of the radiative force, the velocity gradient of both components decreases (see KK0 and the discussion in OP), and, in addition, $G'(\Delta v_0) < 0$. As has already been shown in Sect. 4.2 (see Fig. 3), the flow is unstable in this region.

In the outermost parts of the wind the relation $G'(\Delta v_0) > 0$ holds again and clearly, the wind is stable there. However, because the wind is unstable upstream where $G'(\Delta v_0) < 0$, the instabilities from that unstable region may disseminate and influence the stability of the outermost parts of the wind. Such effects could be studied using hydrodynamical simulations.

Summarizing, there are three regions in the wind of this B5 star. The innermost and outermost parts of the wind are stable against perturbations larger than the Sobolev length, whilst the “middle” part of the wind is unstable (see Fig. 4).

The new slow waves that appeared in the stable solution for a dense wind of an O star (cf. Sect. 4.1) are also present in the stable parts of the wind of a B5 star. For the inner region of stability these waves may be both forward and backward with a special case of “frozen-in” waves for $\kappa = \kappa_0$ where $\Re(\omega) = 0$. Similar to the case of an O star, the value of κ_0 decreases for increasing radii. These waves are also present in the outer stability region, but in this case these waves are purely forward.

4.4. The stability of a B5 star model with normal friction

Finally, we studied the stability of a wind model of a B5 star with $q_i = 2q_{\text{p}}$, which is a bit closer to real winds of B5 stars, at the point where $v_{\text{ri}} \approx 290 \text{ km s}^{-1}$. At this specific point $x_{\text{ip}} \approx 1.4$ and thus, the flow is unstable there. The results of this calculation are similar to those displayed in the Fig. 3. All imaginary roots are negative; the flow is unstable at this selected point. The analysis presented in the preceding section is valid also for this case.

5. Conclusions

We showed that two-component isothermal radiatively driven stellar wind is unstable in the case when friction affects the overall structure of the wind, i.e. when the drift velocity between both components is sufficiently large. Strictly speaking, the wind is unstable if the argument of the Chandrasekhar function is larger than the value for which the maximum of the Chandrasekhar function is reached. For this case so-called ion runaway instability occurs. In the opposite case, when the wind is well

coupled, the Abbott waves (for large scale perturbations) in the wind are stable. Putting these two cases together, stationary wind solutions obtained by KK0 for the case when the drift velocity increases to such values that the Chandrasekhar function passes through the point with its maximum value (i.e. it is decreasing and its derivative is negative) *are not stable*. Note that the region of instability falls within the region of the abrupt decrease of the velocity gradient in the solution found by KK0.

In the real case the obtained large growth rate of the instability will be probably reduced by the energy dissipation via frictional heating. Nevertheless, the inclusion of frictional heating will probably not alter the presence and the overall picture of instability for high drift speeds. However, it is not clear whether the ionic component escapes the star separately (as proposed Springmann & Pauldrach 1992), because the ionic Abbott waves have only modest spatial growth rate (see OP). Hydrodynamical simulations are necessary to resolve this problem. However, it is questionable whether the Sobolev approximation may be used for such calculations. The Sobolev approximation was at the edge of its validity during the calculations of KK0. If the ionic component leaves the star separately, then the Sobolev approximation can be used thanks to a large velocity gradient of absorbing ions after the decoupling (see KKI). On the other hand, if the decoupling process is more complex with modest velocity gradients, we may move beyond the region of validity of the Sobolev approximation.

More complete dispersion relations for a two-component flow should be derived with the inclusion of the short-wavelength perturbations. In the one-component case these perturbations lead to the well-known radiatively driven wind instability (MacGregor et al. 1979; Carlberg 1980; Owocki & Rybicki 1984). When such perturbations on a scale below the Sobolev length are included, then the onset of a two-component instability occurs even below the maximum of the Chandrasekhar function (see OP).

The existence of the two-component instability could also lead to frictional heating of the wind up to temperatures of the order of 10^6 K (cf. KKII). Such heating could explain the enhanced X-ray activity of many B-stars. A similar mechanism of X-ray generation was also proposed by Porter & Drew (1995) and OP. Unfortunately, in the latest numerical models of a three-component nonisothermal wind of B stars the velocity difference is too low to allow for such ion runaway instability (except for extremely low density winds). On the other hand these results are based on a slightly artificial dependence of the radiative force on the temperature and more advanced calculations can alter this result.

In a case of a wind where two-component effects are not important (an O star wind), the two-component stability analysis enabled us to find more types of waves than the classical one-component analysis of Abbott (1980). In addition to the original stable Abbott waves, there exist heavily damped ionic waves and very slow waves with

very weak damping. The latter waves may move in both directions with respect to the wind or they may be static in the comoving fluid frame. Such slow waves resemble “frozen-in” wavy pattern of approximately $\sim 10^7$ cm.

Acknowledgements. The authors would like to thank to Dr. Achim Feldmeier for his valuable comments on the manuscript. This research has made use of NASA’s Astrophysics Data System Abstract Service (Kurtz et al. 2000; Eichhorn et al. 2000; Grant et al. 2000). This work was supported by a grant GA ĀR 205/01/0656, by a grant GA AV ĀR A3003805, and by projects K2043105 and AV0Z1003909.

References

- Abbott, D. C. 1980, *ApJ*, 242, 1183
 Abbott, D. C. 1982, *ApJ*, 259, 282
 Accomazzi, A., Eichhorn, G., Kurtz, M. J., Grant, C. S., & Murray, S. S. 2000, *A&AS*, 143, 85
 Babel, J. 1995, *A&A*, 301, 823
 Carlberg, R. G. 1980, *ApJ*, 241, 1131
 Castor, J. I., Abbott, D. C., & Klein, R. I. 1975, *ApJ*, 195, 157 (CAK)
 Dreicer, H. 1959, *Phys. Rev.*, 115, 238
 Eichhorn, G., Kurtz, M. J., Accomazzi, A., Grant, C. S., & Murray, S. S. 2000, *A&AS*, 143, 61
 Feldmeier, A. 1998, *A&A*, 332, 245
 Feldmeier, A., & Shlosman, I. 2000, *ApJ*, 532, L125
 Feldmeier, A., & Shlosman, I. 2001, *ApJ*, 564, 385
 Friend, D. B., & Abbott, D. C. 1986, *ApJ*, 311, 701
 Grant, C. S., Accomazzi, A., Eichhorn, G., Kurtz, M. J., & Murray, S. S. 2000, *A&AS*, 143, 111
 Jenkins, M. A., & Traub, J. F. 1970, *SIAM J. Numer. Anal.*, 7, 545
 Krtićka, J. 2001, Ph.D. Thesis, Masaryk University Brno
 Krtićka, J., & Kubát, J. 2000, *A&A*, 359, 983 (KK0)
 Krtićka, J., & Kubát, J. 2001a, *A&A*, 369, 222 (KKI)
 Krtićka, J., & Kubát, J. 2001b, *A&A*, 377, 175 (KKII)
 Kurtz, M. J., Eichhorn, G., Accomazzi, A., et al. 2000, *A&AS*, 143, 41
 Lucy, L. B. 1982, *ApJ*, 255, 286
 Lucy, L. B. 1984, *ApJ*, 284, 351
 Lucy, L. B., & Solomon, P. M. 1970, *ApJ*, 159, 879
 Lucy, L. B., & White, R. L. 1980, *ApJ*, 241, 300
 MacGregor, K. B., Hartmann, L., & Raymond, J. C. 1979, *ApJ*, 231, 514
 Owocki, S. P. 1992, in *The Atmospheres of Early-Type Stars*, ed. U. Heber, & C. S. Jeffery, *Lecture Notes Phys.* 401 (Springer Verlag Berlin), 393
 Owocki, S. P., & Cohen, D. H. 1999, *ApJ*, 520, 833
 Owocki, S. P., & Puls, J. 2002, *ApJ*, 568, 965 (OP)
 Owocki, S. P., & Rybicki, G. B. 1984, *ApJ*, 284, 337
 Owocki, S. P., & Rybicki, G. B. 1985, *ApJ*, 299, 265
 Owocki, S. P., & Rybicki, G. B. 1986, *ApJ*, 309, 127
 Owocki, S. P., & Rybicki, G. B. 1991, *ApJ*, 368, 261
 Pauldrach, A., Puls, J., & Kudritzki, R. P. 1986, *A&A*, 164, 86
 Porter, J. M., & Drew, J. E. 1995, *A&A*, 296, 761
 Rybicki, G. B. 1987, in *Instabilities in Luminous Early Type Stars*, ed. H. J. G. L. M. Lamers, & C. W. H. de Loore (D. Reidel Publ. Comp., Dordrecht), 175
 Rybicki, G. B., Owocki, S. P., & Castor, J. I. 1990, *ApJ*, 349, 274
 Springmann, U. W. E., & Pauldrach, A. W. A. 1992, *A&A*, 262, 515